Paleomagnetic investigation of Late Quaternary sediments of South San Francisco Bay, California

J. W. Hillhouse
U.S. Geological Survey
345 Middlefield Road
Menlo Park, Ca. 94025

U.S. Geological Survey
OPEN FILE REPORT 77-457

Abstract

Paleomagnetic inclinations of the Late Quaternary sediments of South San Francisco Bay were determined from bore hole samples collected near Dumbarton Bridge. The sediments consist of estuarine muds and nonmarine sand deposits, floored by bedrock of the Mesozoic Franciscan Formation. Beneath Dumbarton Bridge the entire sedimentary fill is normally polarized; therefore, the fill postdates the Brunhes-Matayama polarity reversal (700,000 y. B.P.). Magnetic time lines such as the Mono Lake excursion (24,000 y. B.P.) and the reversed Blake event (110,000 y B.P.) were not found in this bore hole. In addition to Holocene and modern deposits of San Francisco Bay, an older estuarine unit occurs in the stratigraphic section. The older unit was deposited during a period of high sea level, tentatively correlated with the Sangamon interglacial period. Because evidence of the Blake event is not present in the older estuarine unit, the proposed age of this unit could not be confirmed. Although the Holocene estuarine deposits of South San Francisco Bay carry stable remanent magnetization, a reliable record of geomagnetic secular variation could not be recovered because the water-saturated sediment was deformed by drilling.

Introduction

This report summarizes paleomagnetic measurements obtained from Late Quaternary sediments in the southern lobe of San Francisco Bay. Paleomagnetic directions were determined from core samples recovered from a bore hole near the western end of Dumbarton Bridge in San Mateo County, California (fig. 1). The 180-m bore hole penetrated the entire sedimentary fill, which consists of estuarine muds and fluvial sands, floored by bedrock of the Mesozoic Franciscan Formation. Several intervals of estuarine deposits in addition to the modern deposits of San Francisco Bay are represented in the core. The sea has invaded the basin repeatedly, following eustatic rises in sea level and, to a lesser degree, in response to tectonic subsidence of the basin. The estuarine sediments are interrupted by intervals of sand and gravel that represent periods of fluvial sedimentation and erosion when the sea was exluded from the basin.

I attempted to correlate these sediments with the geomagnetic polarity time scale in order to determine the maximum age of the basin and to date the estuarine periods. Another objective was to assess the suitability of the Holocene bay sediments for determinations of secular variation, the fine-scale fluctuations of the geomagnetic field.

Geologic setting and stratigraphy

The Late Quaternary sediments of South San Francisco Bay occupy a depression roughly bounded by the northern Santa Cruz Mountains on the west and the Diablo Range on the east (fig. 1). The floor of the basin probably consists of Mesozoic rocks of the Franciscan Formation; however, some parts of the basin may be floored by bedrock of Tertiary age. Franciscan rocks crop out near both ends of the Dumbarton Bridge, suggesting that the sediments sampled for paleomagnetism were deposited directly on Franciscan basement (Jennings and Burnett, 1961).

The stratigraphy of the bay deposits has been determined from a large number of bore holes contracted by the California Division of Bay Toll Crossings for studies of bridge foundations. This geologic information is summarized by Atwater, Hedel, and Helley (1976), the source of the following discussion. A stratigraphic cross-section based on bore holes near the Dumbarton Bridge is shown in Figure 2. From oldest to youngest the stratigraphic units consist of: (1) Alluvial and estuarine deposits (Qpa); Late Quaternary. (2) Estuarine deposits (Qpe), Late Quaternary (Sangamon?). (3) Alluvial deposits (Qpha); Late Quaternary-Holocene. (4) Alluvial deposits (Qha); Holocene. (5) Estuarine deposits (Qhe); Holocene and Recent. Seismic profiles combined with bore hole data indicate that the maximum thickness of the sedimentary fill near Dumbarton Bridge is 180 m (Hazelwood, 1976).

The oldest unit, Qpa, consists of alternating layers of sand and clayey silt, representing brief periods of fluvial and estuarine sedimentation. The clayey silts contain ostracods, indicative of brackish or freshwater conditions. Away from the axis of the bay, Qpa grades into coarse alluvial material which may be correlative with the upper part of the Santa Clara Formation, exposed in the low hills to the west (Dibblee, 1966; Lajoie and others, 1974). In other parts of the San Francisco Bay area, deposits named Qpa are much older than the deposits beneath Dumbarton Bridge. These older sediments include the lower beds of the Santa Clara Formation and the Merced Formation. An ash that correlates with the Merced tuff (approximately 1 million years old on the basis of K-Ar and fission track dating), was discovered in Qpa in a borehole near Hunters Point, 35 km northwest of Dumbarton Bridge. The ash occurs 87 m below sea level. The absence of this ash in the 180-m Dumbarton core is probably due to tectonic deformation or erosion in the basin. Consequently,

at Dumbarton Bridge sediments that are younger than the Merced ash lie below the level of the ash as measured at Hunters Point.

The oldest well-developed estuarine unit, Qpe, consists of approximately 15 m of clay and silt containing abundant estuarine pelecypods. Although this unit has not been dated directly, it has been tentatively correlated with the Sangamon interglacial period (70,000-130,000 y. B.P.), known from terrestrial soil horizons (Atwater and others, 1976). During the Sangamon, climatic amelioration melted the glacial ice and raised the level of the sea, as evidenced by a high-standing wave-cut terrace along the California coast. The areal extent of the Sangamon(?) estuary was comparable to that of modern San Francisco Bay.

Fluvial sediments (Qpha) that overlie the older estuarine deposits indicate the retreat of sea water from the basin, probably due to a low stand of the sea. As the shore migrated oceanward and the base level lowered, these deposits were dissected by the streams which had previously supplied sediment to the estuary. This unit correlates with the Wisconsin glacial period of latest Pleistocene age on the basis of radiocarbon-dated (19,000-23,600 ^{14}C y.B.P.) plant fossils found near Mountain View (Atwater and others, 1976).

The Holocene and Recent estuary deposits (Qhe) reflect the rapid eustatic increase in sea level which began approximately 11,000 years ago at the end of the Wisconsin glaciation. Temporal changes of sea level in South San Francisco Bay have been estimated from radiocarbon-dating of fossil plants that, during growth, are restricted to a narrow zone near mean sea level. These levels have been corrected for subsidence due to compaction and isostasy. The evidence indicates that the rising sea entered the Golden Gate 10,000-11,000 years ago and the advancing estuary reached the site of Dumbarton Bridge

approximately 8,000 years ago (Atwater and others, 1976). Since that time, approximately 15 meters of clay and silt, containing abundant peat and invertebrate shells, has accumulated in the southern part of the bay.

The paleomagnetic correlation method

Paleomagnetic correlation of sediments can be applied to strata which are younger than 6.5 million years, the interval spanned by the geomagnetic polarity time scale (Cox, 1969; McDougall and others, 1977). Successful application of this dating technique requires a nearly complete time-stratigraphic record, combined with supporting paleontologic or radiometric data. As a dating tool for Late Quaternary sediments paleomagnetism is severely limited because the geomagnetic field has maintained normal polarity nearly continuously since the Brunhes-Matuyama polarity transition, approximately 700,000 years ago. Attempts have been made to date sediments that are within the range of radiocarbon dating (0-40,000 years) using secular variation, the fine-scale fluctuations of the geomagnetic field. Secular variation curves are only valid within relatively small regions (an approximate radius of 500 km), and adequate calibration curves, derived from radiocarbon dating, have not yet been developed.

During the long Brunhes epoch, the magnetic field has briefly departed from normal polarity. These departures, which include excursions and short reversals, are potentially useful in dating the Dumbarton core. The oldest of these time lines is the Blake event, a brief geomagnetic reversal which occurred approximately 110,000 years ago (Smith and Foster, 1969). This reversal is well-documented by cores taken in the Caribbean Sea and the western North Atlantic Ocean. Because the event has not been found outside this region, it may not be a global time line (Denham, 1976). In the Caribbean,

the Blake event occurs within the X faunal zone, an interval characterized by warm water species of foraminifera (Smith and Foster, 1969; Ericson and others, 1961). The age of the Blake event was extrapolated from radiometric dates (Th^{230}, Th^{231}, and Pa^{231}:Th^{230} methods) determined from Caribbean core Vema 12-122 (Broecker and others, 1968). Because sedimentation within San Francisco Bay may be directly related to climatically controlled changes in sea level, I have summarized paleotemperature data (Foraminifera zones and O^{18} fluctuations) obtained from deep sea cores, showing the time relation between these indicators and the Blake event (fig. 3).

Numerous brief reversed events and geomagnetic excursions have been reported from the interval 10,000-30,000 years B.P. However, evidence from only one of these events, the Mono Lake excursion (24,000 B.P.), is well-documented in the western U.S. region. The excursion is found at several sites within the deposits of Mono Lake (Denham and Cox, 1971; J. C. Liddicoat, personal communication, 1976). Although the polarity of the field did not reverse completely during this event, the virtual geomagnetic pole attained a maximum displacement of 90 degrees from its normal position. The Mono Lake excursion provides a sharp magnetic marker horizon; of course its accuracy as a dating tool depends on the validity of its age-determination, extrapolated from two radiocarbon-dated ostracod horizons within the Mono Lake deposits. Unfortunately, this excursion was very brief (its stratigraphic thickness is less than 50 cm), so that in studies of other Late Quaternary deposits the excursion can easily be missed, either by incomplete sampling or by integration of the depositional remanent magnetization (DRM) due to bioturbation.

Paleomagnetic sampling of the Dumbarton Core

The drill site is located in a reclaimed area 0.5 km west of the west end of Dumbarton Bridge in San Mateo County (fig. 1). Drilling and logging

of the core was carried out by personnel of the Engineering Geology Branch of the U.S. Geological Survey. Information concerning the core can be obtained from:

Mike Bennett
Engineering Geology Branch
USGS
345 Middlefield Road
Menlo Park, Ca. 94025

The upper 30 m of the core were obtained with a Shelby tube corer, 8.9 cm (3.5 in) in diameter and 76 cm long. Tops of the core segments were carefully marked, but no effort was made to preserve the original orientations (declinations) of the segments. The lengths of the wet sediment slugs were compressed a small but unknown amount during extrusion from the Shelby tube. At a depth of 30 m, use of the Shelby tube was discontinued, and the remainder of the core was obtained with a MX wireline sampler. This sampler has an inside diameter of 4.78 cm (1 6/7 in) and is 1.5 m long.

Difficulties due to down-hole slumping temporarily halted the drilling at a depth of 55 m. Several months later the drill rig was moved and the hole was restarted approximately 1 m away from the original site. Coring was resumed at 60 m, and was continued to the base of the sedimentary fill at 180 m. During the drilling operation, recovery of sediment averaged 80 percent in clayey layers and about 20 percent in sandy layers.

The paleomagnetic samples, with volumes of approximately 6 cm^3, were cut from the core with a taut-wire tool. The vertical interval between samples averaged 30-50 cm in clayey layers of the upper 55 m of the core; however, samples were not collected in the sandy layers because the material was considered unsuitable for the paleomagnetic study. Below the 55-m level, paleomagnetic samples were taken at 2-3 m intervals. This lower segment of

the core had been split prior to the paleomagnetic sampling, and a 1-cm thick strip, intended for radiography, had been removed from the center of each slug. Therefore, these particular oriented samples were taken from possibly disturbed material near the outer surface of the core; whereas, samples in the core's upper 55 m were taken from the relatively undisturbed material in the center of the core. For this reason, magnetic directions from the lower samples are only reliable as indicators of polarity, not as records of secular variation.

The core log and the core's relation to the stratigraphy developed by Atwater, Hedel, and Helley (1976) are shown in figure 4.

Paleomagnetic Results

Intensities of natural remanent magnetization (NRM), as determined with a cryogenic magnetometer, range between 10^{-4} and 10^{-2} A/m for these samples (Table 1). In general, the intensities of NRM are low in the uppermost mud unit, and are highest in units containing silt and fine sand. One pilot specimen was progressively demagnetized in alternating fields up to 40 mT, in order to determine the optimum cleaning field for the remaining specimens. Changes in intensity and magnetic direction as functions of alternating field strength are shown for the pilot specimen in Figure 5. Systematic directional changes ceased after treatment in 10 mT; large random changes in direction became apparent after treatment in 20 mT. Therefore, I selected 15 mT as the optimum cleaning field. Compared to the original NRM's of these samples, the magnetizations were typically reduced by a factor of two during the demagnetization treatment.

The paleomagnetic results are grouped according to their stratigraphic positions in the core: 1) Holocene estuarine deposits (Qhe: 0-15 m depth), representing the latest interval of estuarine sedimentation. 2) Sangamon(?)

estuarine deposits (Qpe: 29-54 m depth), an interval of estuarine sediment that underlies alluvial deposits (Qpha) of Wisconsin age. 3) Oldest estuarine and fluvial deposits (Qpa: 68-180 m depth), sampled for determination of polarity only.

Two radiocarbon analyses determined from organic matter in the Holocene mud (Qhe) yielded ages of 3070 $\pm$ 90 years (6 m depth) and 4980 $\pm$ 130 years (12 m depth). A third radiocarbon age of not less than 37,600 years was obtained from wood within the sandy beds (Qpha) at a depth of 16 m. Because other data indicate that the southern limit of San Francisco Bay reached the drill site about 8000 years ago, the radiocarbon ages indicate a depositional hiatus between 13-m and 16-m depth levels. Therefore, a record of the Mono Lake excursion (24,000 years B.P.) was not expected in this core.

For the most part, inclinations within the Holocene estuary deposits (Qhe) are scattered about +57°, the inclination expected from an axial dipole of normal polarity (fig. 6). However, inclinations determined from adjacent specimens from the same horizon show poor internal consistency. The large amount of scatter (up to 50 degrees) is probably caused by deformation of the sediment during coring rather than by a flaw in the natural paleomagnetic recording process. Radiographs indicate major deformation of the bedding planes in some segments. The water content of this mud (fig. 6) ranges between 60 and 90 percent, which accounts for the extreme plasticity of the core segments.

Anomalously low inclination, observed in a single horizon at a depth of 9 m, may reflect real secular variation, but probably is due to plastic deformation of the core. During coring, fragments of oyster shells, which are abundant at this depth, may have been dragged along the inner wall of the core barrel, causing deformation of the water-saturated sediment. Because

the oyster shells are extremely abundant in this part of the core, it was not possible to collect additional samples in the 5-12 m depth interval, and thus find corroborating evidence for the anomalously low inclination at 9-m depth.

Laboratory experiments in which sediment was redeposited in a simulated estuarine environment have shown that the sediment acquires stable remanent magnetization parallel to the ambient magnetic field (Graham, 1974). The sediment used in this study was collected from a modern tidal "mud flat" near Dumbarton Bridge. After the redeposition experiment was completed, the pan containing the sediment was flooded and drained several times in order to simulate tides. The initial direction of magnetization remained constant during the repeated wet and dry cycles, despite the application of a reversed ambient magnetic field. Graham concluded that the modern bay deposits were accurately recording the earth's magnetic field, and therefore, the Holocene deposits were potentially useful for refining the record of geomagnetic secular variation. However, the magnetization may become permanently locked-in at a considerable depth (~ 1 m) below the upper surface of the sediment, because burrowing organisms thoroughly churn the upper layer.

My study shows that weak but stable magnetization is present throughout the Holocene estuary deposits. Unfortunately, the water-saturated sediment was extremely deformed by the coring operation, hence a reliable record of secular variation was not recovered from this core. Better results might be obtained in the future if a sampler with a larger diameter is utilized.

Wherever possible, the Sangamon(?) estuarine unit (Qpe: 29-54 m depth) was sampled at close intervals, the object being discovery of the reversed

Blake event. Because the oceanic record indicates that the Blake event occurred during the warm X (foraminifera) interval, possibly correlative with the terrestrial Sangamon period, the older estuarine unit (Qpe) appeared to be the best section in which to search for the Blake event. As shown in figure 6, the entire section, except for a possibly disturbed horizon at 42.6 m, is normally polarized. There is no evidence of the Blake event in the older estuarine unit. If we start from the assumption that the Blake event is a reversal of global extent, then its absence from the Dumbarton core has several possible explanations: 1) The estuarine unit (Qpe) developed some time before or after the Blake event. 2) The event was missed because it occurred within a gap between paleomagnetic samples or during a depositional hiatus. The Blake event, believed to be approximately 5000 years long, should span 1-5 m of section, on the basis of the Holocene estuarine sedimentation rate. Gaps exceeding one meter in thickness appear in the older estuarine unit, and could not be avoided, because the recovery of sediment was poor in some intervals. 3) Burrowing organisms may have thoroughly reworked the sediment, so that any record of the Blake event was integrated away.

The lowest unit (fig. 4) (Qpa) is entirely of normal polarity. The absence of reversed horizons strongly suggests that the entire sedimentary fill post-dates the Brunhes-Matuyama polarity reversal, approximately 700,000 y. B.P.

Conclusions

1) The Holocene estuarine deposits (Qhe) of South San Francisco Bay possess stable remanent magnetization, but extreme deformation, produced in the water-saturated sediment by coring, spoiled the record of secular variation.

2) Because the Blake event (110,000 y. B.P.) was not found in this core, the proposed Sangamon age of the older estuarine unit (Qpe) was not confirmed.

3) The entire sedimentary fill beneath Dumbarton Bridge post-dates the Brunhes-Matuyama polarity reversal (700,000 y. B.P.).

Bibliography

Atwater, B. F., Hedel, C. W., Helley, E. J., (in press), Late Quaternary depositional history, Holocene sea-level changes, and vertical crustal movement, South San Francisco Bay, California, U.S. Geol. Survey Prof. Paper, No. 1014.

Broeck er, W. S., Thurber, D. L., Goddard, J., Ku T. L., Matthews, R. K., and Mesolella, K. J., 1968, Milankovitch hypothesis supported by precise dating of coral reefs and deep-sea sediments, Science, v. 159, p. 297.

Broecker, W. S. and Van Donk, J., 1970, Insolation changes, ice volumes, and the O^{18} record in deep-sea cores, Rev. Geophys. and Space Phys., v. 8, p. 169-198.

Cox, A., 1969, Geomagnetic reversals, Science, v. 163, p. 237-245.

Denham, C. R., 1976, Blake polarity episode in two cores from the Greater Antilles Outer Ridge; Earth Planet. Sci. Lett., v. 29, p. 422-434.

Denham, C. R. and A. Cox, 1971, Evidence that the Lashamp Polarity event did not occur 13,300-30,400 years ago, Earth Planet. Sci. Lett., v. 13, p. 181-190.

Dibblee, T. W., Jr., 1966, Geologic map of the Palo Alto 15-minute quadrangle, California: Calif. Div. Mines and Geol., Map Sheet 8, scale 1:62,500.

Emiliani, C., 1966, Paleotemperature analysis of Caribbean cores P6304-8 and P6304-9 and a generalized temperature curve for the past 425,000 years, J. Geol., v. 74, p. 109.

Ericson, D. B., Ewing, M., Wollin, G. A., and Heezen, B. C., 1961, Atlantic deep-sea sediment cores, Geol. Soc. Amer. Bull., v. 72, p. 193-286.

Graham, S., 1974, Remanent magnetization of modern tidal flat sediments from San Francisco Bay, California: Geology, v. 2, p. 223-226.

Hazelwood, R. M., 1976, Contour map and interpretive cross sections showing depth and configuration of bedrock surface, South San Francisco Bay region, California: U.S. Geol. Survey Misc. Field Studies Map, MF 796.

Jennings, C. W. and Burnett, J. L., 1961, Geologic map of California: San Francisco Sheet: Calif. Div. of Mines and Geol., scale 1:250,000.

Lajoie, K. R., Helley, E. J., Nichols, D. R., and Burke, D. B., 1974, Geologic map of unconsolidated and moderately consolidated deposits of San Mateo County, California: U.S. Geol. Surv. Misc. Field Studies Map, MF 575.

McDougall, T., Saemundsson, K., Johannesson, H., Watkins, N., and Kristjansson, 1977, Extension of the geomagnetic polarity timescale to 6.5 m.y.: K-Ar dating, geological and paleomagnetic study of a 3,500-m lava succession in western Iceland: Geol. Soc. Amer. Bull., v. 88, p. 1-15.

Smith, J. D. and Foster, J. H., 1969, Geomagnetic reversal in Brunhes normal polarity epoch: Science, v. 163, p. 565-567.

Table 1. Summary of paleomagnetic results from the Dumbarton Bridge core.

a) NRM and demagnetization results (A.F. = 15mT (150 oe) from first core (0-55 m) and from second core (68-175 m).

b) Results from second core in which the depth interval, 39-46 m, was resampled.

Depth: Depth of specimen below sea level

I: Inclination

D: Declination (relative to split face of core, not true north)

J: Intensity, showing exponent; eg. 3.40-6 = 3.40×10^{-6} emu/cm^3. (10^{-6} emu/cm^3 = 10^{-3} A/m)

Table 1a: Paleomagnetic results from the Dumbarton Bridge Core

Number	Depth(m)	Natural Remanent Magnetization I	D	J	A.F. demagnetization (15 mT) I	D	J
3A-20.8A		71.0	292.2	7.52-7	59.0	341.1	3.53-7
B		48.5	318.6	6.58-7	61.1	310.4	3.74-7
4A-18.8A	1.28	52.6	68.1	1.34-6	62.5	47.5	4.04-7
B		54.4	37.1	1.37-6	42.0	58.5	5.69-7
5A-20.8A	1.81	70.5	194.2	2.26-6	51.2	114.2	1.00-6
B		46.5	146.2	2.46-6	41.5	125.6	1.20-6
6A-14.8A	2.25	53.5	102.2	2.70-6	59.5	29.5	1.70-6
B		62.6	103.1	5.31-6	52.2	85.2	2.43-6
7A-14.8A	2.75	54.6	298.3	2.12-6	69.5	37.0	4.99-7
B		60.8	263.4	3.14-6	84.1	302.7	6.44-7
8A-13.8A	3.23	34.9	3.7	8.22-6	29.1	14.4	4.01-6
B		48.4	0.0	3.90-6	43.8	15.9	1.09-6
9A-23.8A	3.94	38.8	138.0	1.53-6	29.1	118.8	7.25-7
B		56.8	159.4	1.49-6	40.0	122.1	5.94-7
10A-14.8A	4.35	59.4	106.3	1.15-5	64.5	110.9	6.55-6
B		59.2	6.3	9.94-6	57.3	38.0	5.29-6
11A-12.8A	4.83	33.3	3.7	5.56-6	25.1	6.7	2.30-6
B		67.0	16.1	4.85-6	72.0	348.6	2.18-6
18A-12.8A	8.83	17.0	208.0	8.29-7	13.7	140.4	2.91-7
B		12.0	200.1	8.28-7	12.2	180.3	2.64-7
19B-.7.2A	9.55	20.1	40.4	9.66-7	8.1	53.6	4.20-7
B		67.3	75.9	9.12-7	43.7	88.3	3.64-7
23C-44.8A	11.85	62.9	114.1	2.29-5	63.7	108.3	1.05-5
B		48.7	120.4	3.12-5	49.6	112.9	1.48-5
27B-16.8A	13.21	44.1	278.7	2.43-5	48.5	280.6	1.04-5
B		59.4	204.1	2.79-5	64.1	196.4	1.06-5
28B-39.5A	13.85	55.5	98.5	2.07-5	54.8	99.9	1.18-5
B		54.9	102.4	1.74-5	56.8	96.9	9.55-6
29B-36.8A	14.37	56.3	290.6	2.59-5	58.2	296.3	1.30-5
B		60.4	293.6	2.77-5	60.6	295.3	1.14-5
30A-22.5A	14.73	48.9	140.7	9.01-5	47.9	138.7	5.02-5
B		58.9	164.5	6.77-5	56.2	157.6	3.67-5
48B-34.0A	28.74	66.7	28.5	2.12-5	50.2	30.8	7.17-6
B		73.7	16.9	2.20-5	61.4	31.4	7.52-6
49A-8.0-A	29.48	42.2	324.7	3.12-5	45.5	326.2	1.29-5
B		43.1	315.6	2.39-5	45.6	328.8	1.13-5
49B-38.0A	29.77	45.4	242.4	3.50-5	48.1	246.0	1.20-5
B		46.5	247.4	3.74-5	48.5	250.1	1.41-5
50B-34.5	30.05	64.3	126.8	3.12-5	64.4	113.9	1.39-5
51A-31.0	30.61	31.9	209.4	7.73-5	28.7	206.9	4.41-5
51A-46.0	30.76	56.5	177.0	2.28-5	59.4	165.2	9.62-6
54A-23.0	33.53	58.9	356.4	2.17-5	46.8	5.2	8.80-6
55A-34.0	35.14	61.1	148.0	3.25-5	63.2	134.7	1.54-5
55A-56.0	35.36	67.1	311.0	2.75-5	63.0	332.8	8.71-6
56A-33.0	36.72	55.4	149.4	4.40-5	49.6	127.1	1.38-5
56A-34.0	36.73	69.4	90.6	3.76-5	58.6	64.4	1.26-5
57A-18.0	37.78	76.7	80.2	2.69-6	65.5	62.6	9.75-7
57A-43.0	38.03	72.7	179.0	2.62-6	78.3	217.9	9.88-7
57B-70.0	38.30	70.6	41.7	3.01-6	72.6	44.6	1.06-6
59A-25.0	40.25	66.1	172.3	3.78-6	76.8	182.7	9.91-7

Table 1a - continued

Number	Depth	I_{NRM}	D_{NRM}	J_{NRM}	I_{150}	D_{150}	J_{150}
60C-96.5	42.29	58.9	81.1	1.60-6	47.0	18.9	4.70-7
60B-83.0	42.42	40.5	197.4	2.37-6	35.3	210.9	8.08-7
60B-60.0	42.65	46.6	188.1	1.34-6	46.4	186.3	4.27-7
60A-31.0	42.94	54.8	79.7	2.53-6	46.3	73.4	1.12-6
60A- 5.0	43.20	64.6	273.5	2.26-6	42.7	296.7	5.43-7
62A-11.0	45.27	59.2	122.8	2.37-6	58.2	146.7	8.52.7
62A-32.0	45.47	64.3	4.0	2.50-6	54.7	337.4	9.27-7
62B-63.0	45.77	69.6	186.2	3.50-6	66.4	172.8	7.73-7
62B-100.0	46.15	59.9	23.0	2.82-6	36.4	10.7	9.37-7
64A-14.5	47.58	46.5	288.4	3.10-6	28.8	289.5	1.04-6
64A-50.0	47.92	45.0	335.2	3.07-6	43.1	322.7	1.12-6
64B-65.0	48.05	63.3	119.6	2.89-6	53.3	128.9	7.12-7
64C-93.0	48.36	65.6	339.4	3.72-6	43.7	316.8	8.41-7
64C-120.0	48.62	40.7	289.9	9.19-6	37.6	282.3	3.81-6
64C-135.0	48.77	42.7	291.8	7.33-6	27.8	277.5	3.60-6
66A-32.0	50.42	59.0	150.9	8.73-6	56.5	157.8	2.00-6
66A-49.0	50.59	84.0	24.6	1.50-5	78.0	19.3	2.91-6
67A-5.0	51.15	54.6	228.1	1.40-6	31.8	246.6	6.45-7
67A-32.0	51.42	65.4	169.6	2.84-5	59.6	176.0	1.45-5
68A-47.0	53.07	63.4	244.4	3.45-5	55.1	247.0	1.70-5
68A-48.0	53.08	58.4	232.2	3.45-5	53.2	236.0	1.77-5
68B-66.0	53.25	59.3	102.3	5.31-5	62.4	106.8	2.19-5
68B-86.0	53.46	56.6	100.5	4.46-5	57.0	99.7	1.73-5
68C-101.0	53.61	53.4	95.8	4.13-5	47.9	92.6	1.51-5
84C-115.0	68.75	71.4	341.6	1.36-5	68.1	341.1	8.23-6
86A-12.0	70.57	64.2	119.0	2.73-5	55.1	110.4	1.27-5
90B-58.0	77.08	60.2	182.6	4.16-5	63.8	157.3	1.41-5
94A-27.0	81.47	59.9	152.6	2.28-5	57.2	144.1	1.07-5
96C-84.0	84.94	48.1	259.3	5.57-5	48.6	259.5	1.88-5
98C-94.0	87.94	65.0	120.9	8.97-6	68.4	115.9	3.25-6
100C-105.0	91.25	52.0	189.4	2.31-5	53.1	180.9	9.33-6
104A-15.0	96.25	56.8	107.6	3.00-5	55.9	106.0	1.57-5
110D-133.0	107.73	70.5	320.7	2.49-5	66.5	337.4	9.02-6
112C-74.0	110.14	69.5	139.8	1.47-5	65.7	133.4	4.63-6
114B-50.0	112.90	52.0	139.1	1.05-5	45.2	136.4	3.92-6
116B-72.0	116.12	59.3	312.9	7.97-5	57.5	318.2	6.43-5
118A-96.0	118.68	51.0	73.7	5.93-6	48.0	70.2	5.25-6
119D-86.0	121.06	49.4	22.4	1.57-6	47.2	24.5	9.02-7
121C-1210	124.41	59.0	198.6	4.02-5	59.6	186.3	1.32-5
123A-15.0	126.55	49.6	234.0	2.54-5	50.2	229.9	1.13-5
125A-32.0	131.92	72.0	357.6	1.74-5	68.3	9.1	9.14-6
129A- 5.0	138.20	45.6	174.2	4.83-5	43.1	173.6	3.27-5
130D-141.0	139.91	58.4	150.3	5.10-5	56.2	136.4	2.23-5
132B-63.0	142.13	54.8	325.1	2.93-5	55.6	327.2	1.17-5
134C-86.0	145.26	56.3	105.3	3.42-5	51.3	98.2	2.25-5
137B-53.0	149.85	56.1	176.5	4.11-5	49.0	166.4	1.73-5
138C-39.0	152.17	42.3	171.5	2.21-5	45.9	159.3	1.22-5

Table 1a - continued

Number	Depth	I_{NRM}	D_{NRM}	J_{NRM}	I_{150}	D_{150}	J_{150}
142A-23.0	161.23	52.9	177.0	3.34-5	53.0	168.4	2.04-5
143B-80.0	163.40	56.3	113.0	1.71-5	48.9	107.5	7.23-6
145B-75.0	167.12	59.6	285.4	2.00-5	80.7	286.8	5.04-6
147A-17.0	169.37	48.5	186.6	2.31-6	9.4	185.0	6.10-7
149C-104.0	173.24	53.5	205.8	3.20-6	57.2	252.7	6.07-7
150A-17.0	173.83	30.0	176.4	2.18-6	8.2	183.2	1.00-6
150A-27.0	173.93	-3.6	211.1	6.03-6	-2.7	197.7	2.44-6

Table 1b

Number	Depth	Natural Remanent Magnetization I	D	J	A.F. demagnetization (15 mT I	D	J
75A-14.0	39.12	46.2	42.6	3.40-6	27.6	36.0	1.35-6
75A-22.0	39.22	80.1	356.3	3.93-6	77.7	15.6	1.39-6
75A-32.0	39.32	59.0	292.8	4.06-6	57.9	300.6	1.53-6
75B- 8.0	39.46	67.8	214.9	4.04-6	66.5	221.7	1.31-6
75B-18.0	39.56	59.1	167.4	2.76-6	58.5	177.5	8.27-7
75B-30.0	39.68	66.9	96.7	3.16-6	63.9	96.7	1.11-6
75C- 5.0	39.84	65.2	81.4	3.20-6	57.2	82.8	9.24-7
75C-17.0	39.96	54.9	53.0	3.91-6	52.7	27.3	1.26-6
75C-31.0	40.11	72.2	234.1	4.33-6	57.5	236.4	1.14-6
77A- 8.0	41.68	43.9	283.7	2.72-6	43.1	296.8	1.01-6
77A-17.0	41.77	63.9	31.4	3.88-6	56.3	19.8	1.41-6
77A-29.0	41.89	66.9	147.9	5.67-6	61.3	136.6	1.52-6
77C-107.0	42.67	4.7	279.0	9.16-6	-2.7	262.5	4.86-6
77C-115.0	42.75	66.2	332.6	8.95-6	56.3	346.6	1.53-6
77C-126.0	42.86	65.8	46.5	4.42-6	55.4	55.2	1.61-6
78D- 8.0	43.08	65.0	75.1	1.64-6	58.6	44.5	5.7607
78D-28.0	43.28	72.8	192.7	1.46-6	77.4	239.8	4.97-7
78C-55.0	43.55	72.1	15.5	6.51-6	44.2	19.4	1.32-6
78C-66.0	43.66	60.9	251.4	622-6	45.2	249.3	1.61-6
78B-85.0	43.85	55.2	37.6	3.05-6	40.1	31.9	8.69-7
78A-123.0	44.23	67.4	354.8	1.72-6	56.0	0.4	7.36-7
78A-135.0	44.35	53.7	54.9	2.42-6	36.6	51.8	9.08-7
79A-10.0	44.82	52.7	188.5	4.35-6	44.8	188.2	1.14-6
79A-20.0	44.92	57.5	78.0	3.80-6	54.2	67.6	9.63-7
79A-30.0	45.02	54.5	74.3	3.87-6	48.7	58.2	1.17-6
79B-45.0	45.17	64.6	152.1	3.65-6	64.7	147.4	1.08-6
79B-57.0	45.29	63.6	292.6	3.81-6	55.9	306.2	1.09-6
79B-68.0	45.40	55.1	291.8	1.63-5	35.0	282.7	1.54-6
79B-76.0	45.48	67.2	216.8	1.08-5	60.8	218.9	2.06-6

Figure 1. Geologic map of South San Francisco Bay region, showing location of drill site and cross-section. Geologic units:

1) Q : Quaternary alluvium, terrace, and estuarine deposits.

2) MT: Tertiary and Mesozoic volcanic, sedimentary, and plutonic rocks, undifferentiated.

3) KJf: Mesozoic Franciscan Formation and associated ultramafic rocks.

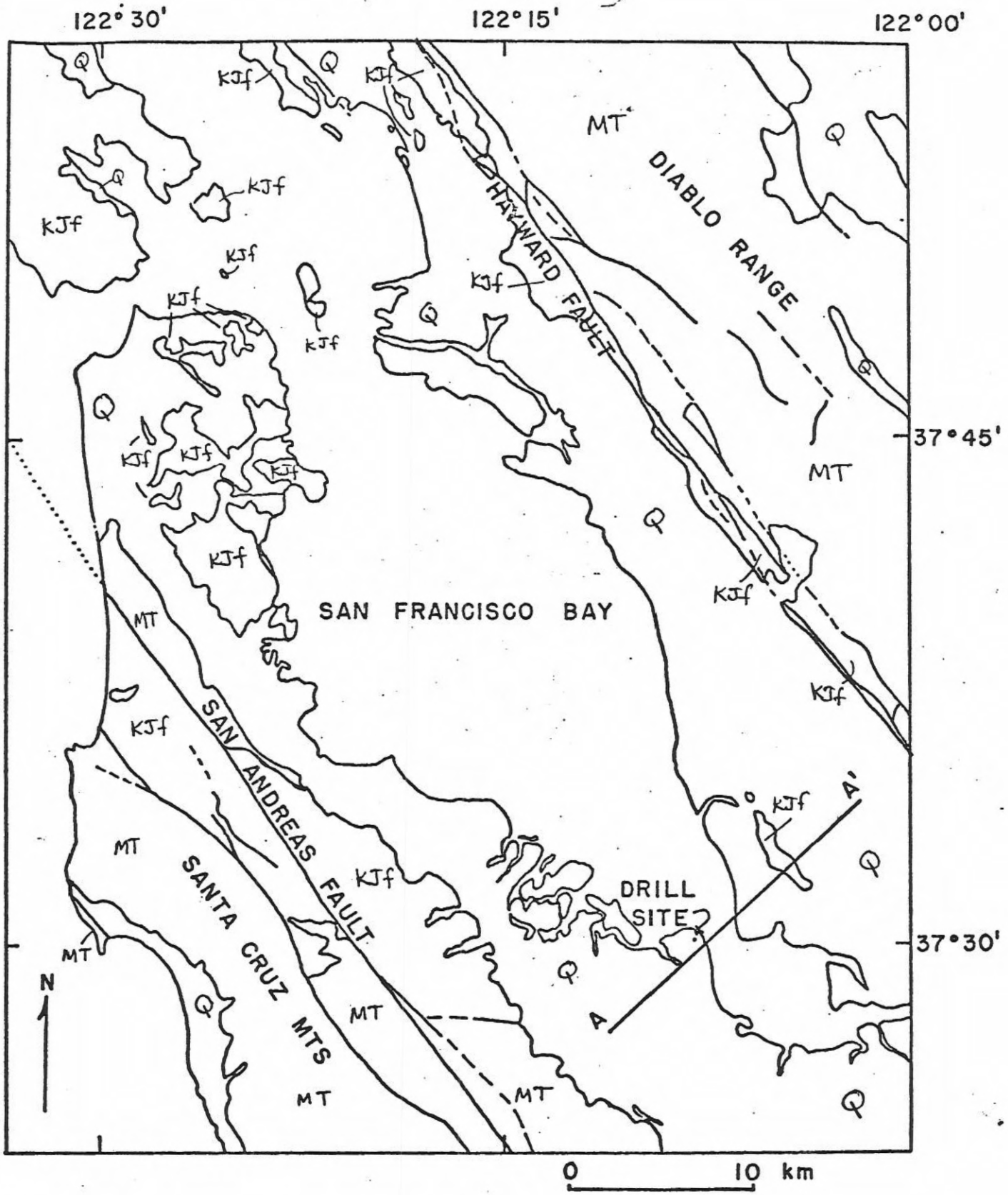
122° 30'
122° 15'
122° 00'
37° 45'
37° 30'
Q
KJf
MT
HAYWARD FAULT
DIABLO RANGE
SAN FRANCISCO BAY
SAN ANDREAS FAULT
SANTA CRUZ MTS
DRILL SITE
A
A'
N
0
10 km

Figure 2. Cross-section (A-A') showing Quaternary deposits penetrated by the borehole near Dumbarton Bridge. Geologic units: 1) Qhe: Estuarine deposits; Holocene and recent. 2) Qha: Alluvium; Holocene. 3) Qpha: Alluvium; late Pleistocene-Holocene. 4) Qpe: Estuarine deposits; late Pleistocene (Sangamon?). 5) Qpa: Alluvium and estuarine deposits; late Pleistocene. 5) KJf: Franciscan Formation; Mesozoic. Basement contour is based on seismic profiles and bore hole data (Hazelwood, 1976).

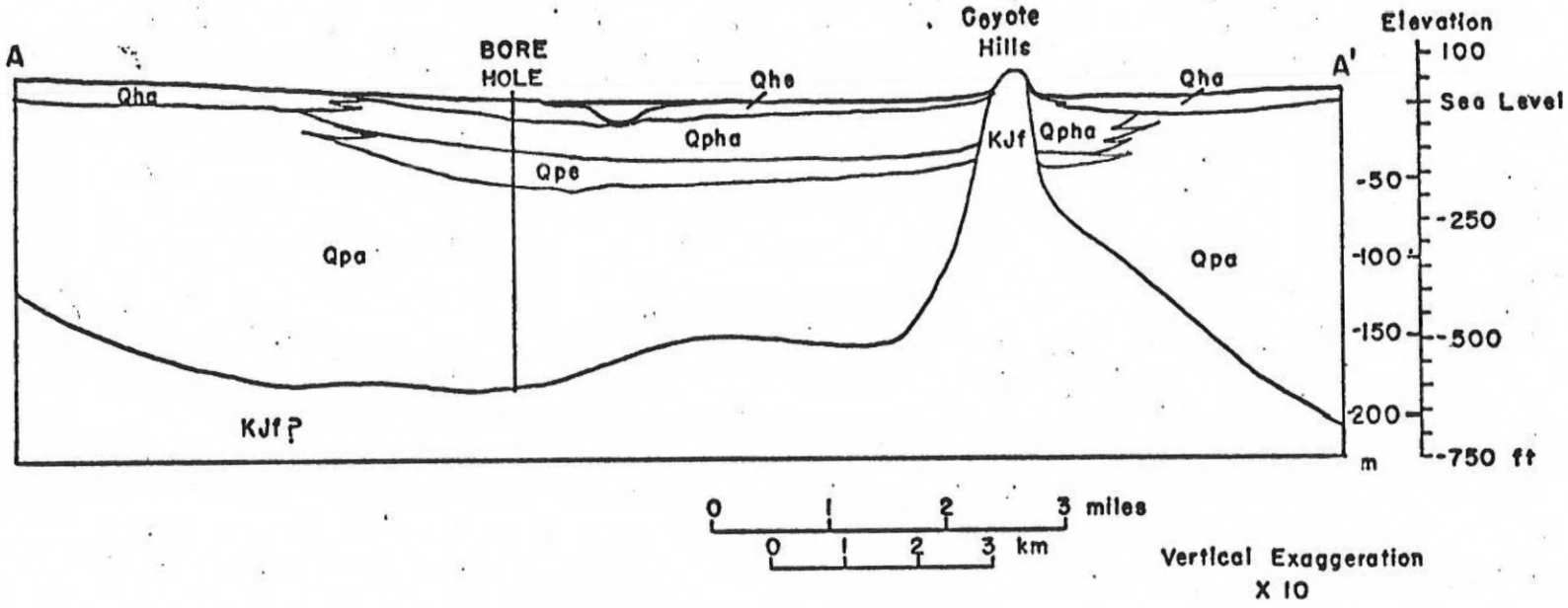
A
BORE HOLE
Coyote Hills
A'
Elevation
100
Sea Level
-50
-100
-150
-200
m
-250
-500
-750 ft
Qha
Qhe
Qpha
Qpe
KJf
Qpa
KJf?
0 1 2 3 miles
0 1 2 3 km
Vertical Exaggeration
X 10

Figure 3. Temporal relation of Brunhes-age magnetic time lines and paleotemperature data from deep-sea sediments. Foraminifera zones are from Ericson, Ewing, Wollin, and Heezen, 1961. Oxygen-18 results are from Emiliani (1966), with dating modified by Broecker and van Donk (1970). Roman numerals shown on sea level curve (Broecker and van Donk, 1970) correspond to marine terraces of the Barbados Is. Cross hatching denotes normal polarity.

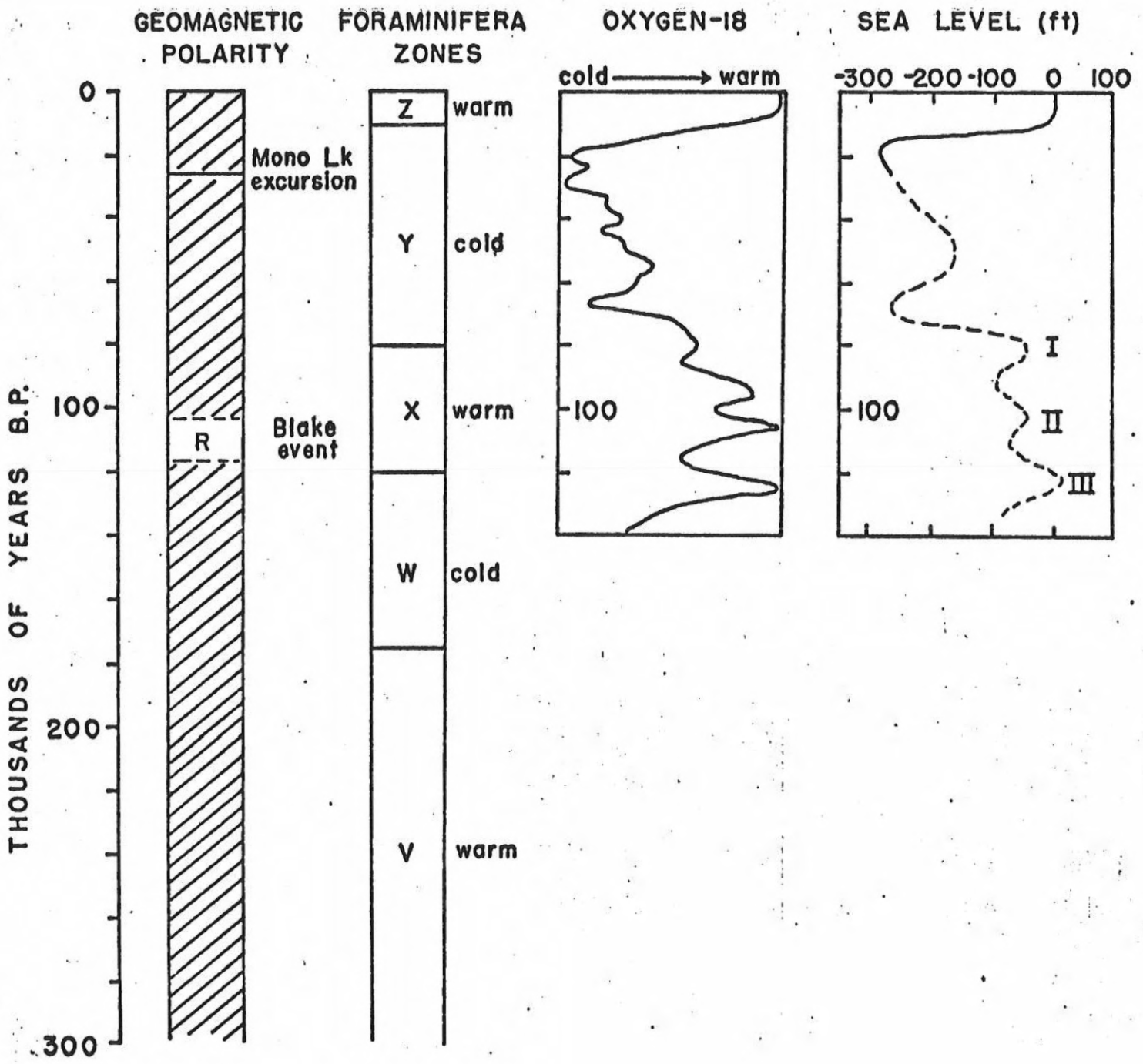
GEOMAGNETIC POLARITY
FORAMINIFERA ZONES
OXYGEN-18
SEA LEVEL (ft)
cold → warm
-300 -200 -100 0 100
THOUSANDS OF YEARS B.P.
0
100
200
300
Mono Lk excursion
R
Blake event
Z warm
Y cold
X warm
W cold
V warm
100
100
I
II
III

Figure 4. Log of Dumbarton core showing radiocarbon-dated horizons, geologic units of fig. 2, and normally polarized horizons sampled in Qpa. Paleomagnetic results from the upper 55 m of the core are shown in fig. 6. Source of radiocarbon dates: 1) 3070 $\pm$ 90 years, oyster shells (USGS 35, Dumbarton west 13B), 2) 4830 $\pm$ 130 years, oyster shells (USGS 36, Dumbarton west 23B), 3)>37,600, wood (USGS 55, Dumbarton west 33B).

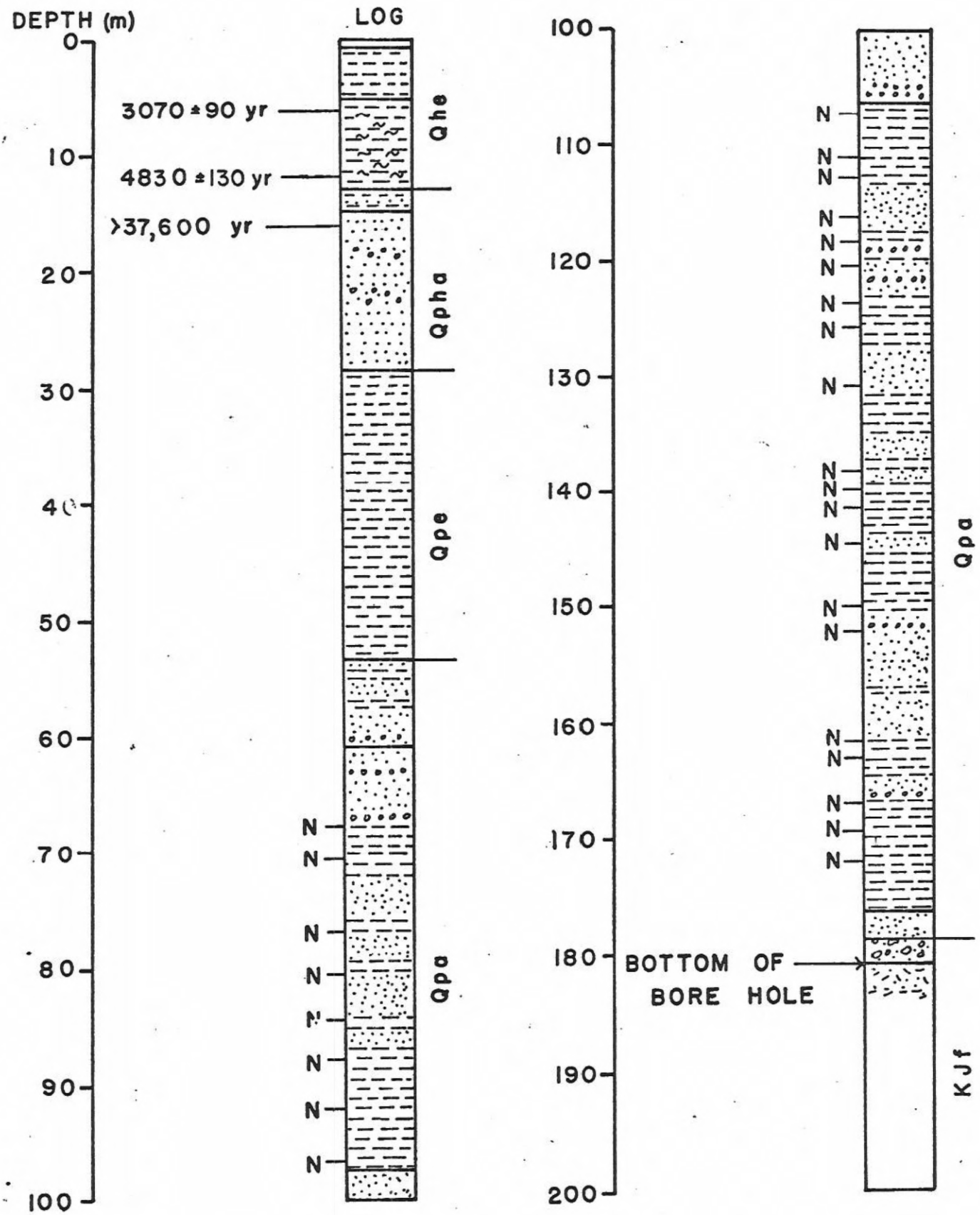
DEPTH (m)
LOG
0
10
20
30
40
50
60
70
80
90
100
3070 ± 90 yr
4830 ± 130 yr
>37,600 yr
Qhe
Qpha
Qpe
Qpa
N
100
110
120
130
140
150
160
170
180
190
200
BOTTOM OF
BORE HOLE
Qpa
KJf

Figure 5. Progressive demagnetization of specimen 6H14.8A. Changes in intensity and magnetic direction are shown for applied alternating fields up to 40 mT (400 oe).

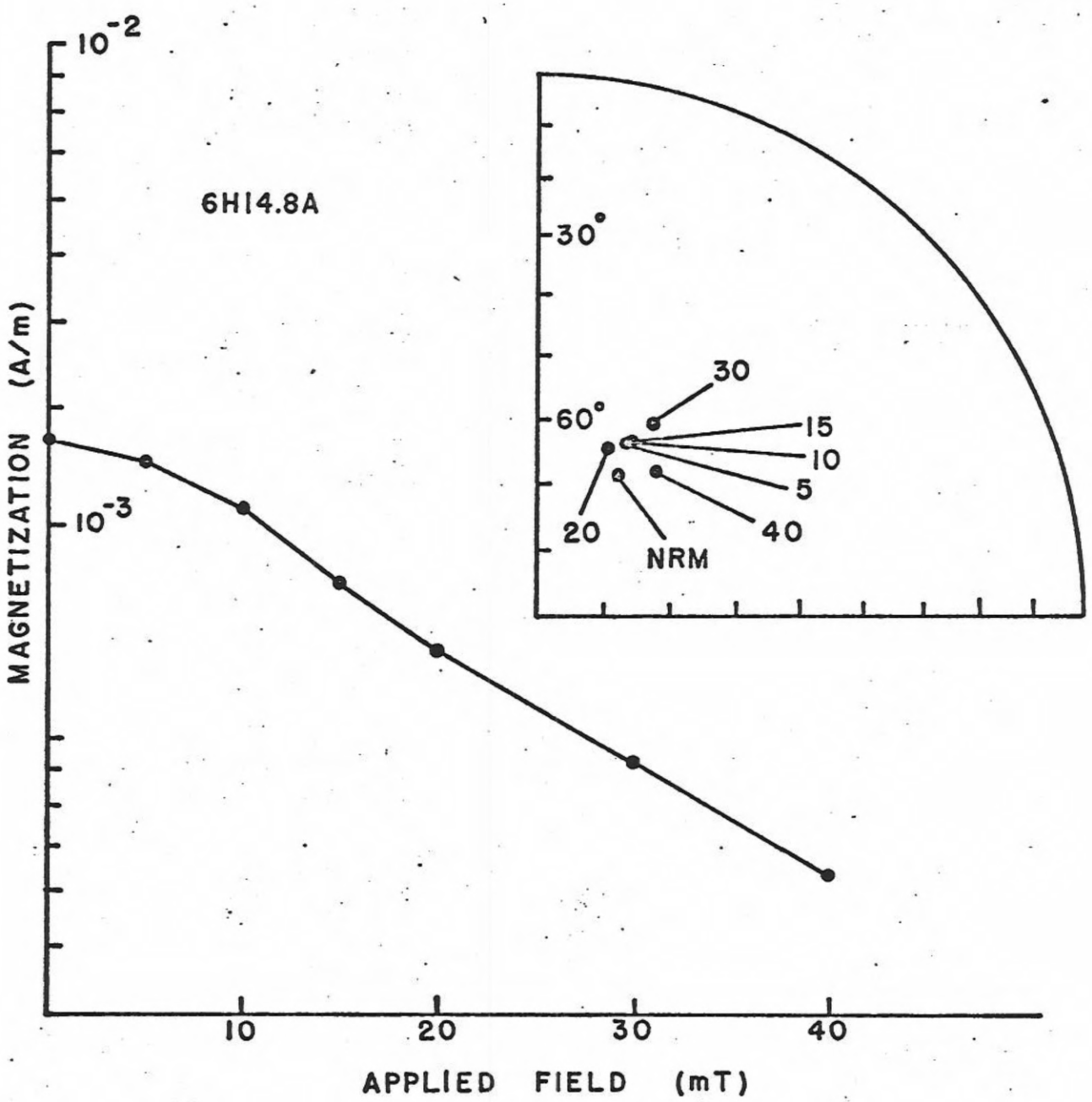
6H14.8A
10^{-2}
10^{-3}
MAGNETIZATION (A/m)
10
20
30
40
APPLIED FIELD (mT)
30°
60°
30
15
10
5
40
20
NRM

Figure 6. Magnetic inclinations of specimens collected from the upper estuarine units. Dots represent first borehole; crosses represent interval resampled in second borehole. Inclination calculated from the geocentric, axial dipole field is shown by the dashed line.